# Expansion and drug elution model of a coronary stent

F. MIGLIAVACCA[§], F. GERVASO[§], M. PROSI[†], P. ZUNINO[†], S. MINISINI[†],

L. FORMAGGIA[†] and G. DUBINI[§]

§LaBS - Laboratorio di Meccanica delle Strutture Biologiche,
Dipartimento di Ingegneria Strutturale,
Politecnico di Milano,
P.zza L. Da Vinci 32, 20133 Milano, Italy

† MOX-Modellistica e Calcolo Scientifico,
Dipartimento di Matematica "F. Brioschi",
Politecnico di Milano,
Via Bonardi 9, 20133 Milano, Italy

**Keywords**: Mathematical model; Coronary stent; Finite element method; Drug elution

**Abstract**

The present study illustrates a possible methodology to investigate drug elution from an expanded coronary stent. Models based on finite element method have been built including the presence of the atherosclerotic plaque, the artery and the coronary stent. These models take into account the mechanical effects of the stent expansion as well as the effect of drug transport from the expanded stent into the arterial wall. Results allow to quantify the stress field in the vascular wall, the tissue prolapse within the stent struts, as well as the drug concentration at any location and time inside the arterial wall, together with several related quantities as the drug dose and the drug residence times.

## 1 Introduction

Arterial diseases like atherosclerosis are the leading causes of death in the industrialized world. They may cause a reduction of the blood flow because of the narrowing or occlusion of the affected arteries. Intravascular stents, which are small tube-like structures, may be driven and expanded into the stenotic artery to restore blood flow perfusion to the downstream tissues. Nowadays, stent implantation is a common procedure with a high rate of success when compared with angioplasty alone [1,2]. However, some limitations are still present and the major ones are those associated with the 'in-stent restenosis' process. When it occurs, the treated vessel may become blocked again. It usually happens within the first 6 months after the initial procedure [3]. Different stages are involved in this process and they can be summarized, as reported by Edelman and Rogers [4], as thrombosis, inflammation, proliferation and remodeling. Many factors have been found to influence the degree of restenosis, such as the degree of damaged endothelial cells and the depth of the injury [5,6], the type of stent expansion (self or balloon expanding, [7]), the design of the stent [8] and the local fluid dynamics [9,10]. The stent deployment inside an artery has many implications on the stresses and deformations in the arterial wall and hence has an impact on the progression of in-stent restenosis. Computational structural analysis has emerged in recent years to investigate the mechanical response to angioplasty and stent placement in the arterial wall [11-17].

Recently, the introduction of drug eluting stents in interventional cardiology practice seemed to bring bare-metal stenting to a rapid decline [18]. In the drug eluting stents a polymeric matrix is added to the stent struts, loaded with a drug which is released after the implant. Clinical trials [19,20] showed a reduction of restenosis when a drug eluting stent is used. However, research has still to be done to define the variables (i.e. strut thickness and shape, pore sizes of the stent coating) of stent geometry influencing the

clinical outcome. Indeed, an effective release of the drug from the coating into the wall depends on many factors, mainly the stent design, the drug and the coating type.

Recently, some computational works considered the convection-diffusion equations to model the spatial and temporal distribution of drug concentration within the vessel wall [21,22]. They demonstrated how numerical simulations are viable tools to study these phenomena. However, to be effective they have to account properly for the expansion of the struts and their interaction with the vascular wall. Indeed, these aspects influence the outcome of the stenting procedure.

The present study aims at showing a possible methodology to investigate the drug elution from a realistic model of a coronary stent. It takes into account the mechanical effects of the stent expansion as well as the effect of drug release from the expanded stent into the arterial wall.

## 2 Materials and Methods

The approach here proposed analyses the stent expansion and the drug elution as two distinct and consecutive phases. During the former phase, a stent is expanded inside an atherosclerotic coronary artery using a large deformation mechanical model by means of the commercial finite element code ABAQUS (Abaqus Inc, RI, USA). In the latter phase, the deformed coronary artery and stent are used as input geometries on which the drug eluting model analysis is carried out. In this case, the numerical solution of the partial differential equations describing the plasma filtration and the mass transport in the arterial wall is obtained by an in-house code (LifeV: a finite element library. http://www.lifev.org).

### *2.1 Stent expansion model*

The stent expansion model is constituted by the coronary artery, the plaque and the stent.

**2.1.1 Coronary artery model.** The artery (Fig. 1) is modelled as a cylinder having a length of 11.68 mm, an internal diameter of 2.15 mm and a thickness of 0.5 mm. It is discretised by means of 6720 8-node linear hybrid brick elements with a corresponding number of nodes of 9120. The hybrid formulation was chosen in order to account for the incompressibility constraint of the material. To describe the mechanical behaviour of the artery, a hyperelastic isotropic constitutive model is adopted as described by Hayashi and Imai [23]. In particular, the constitutive law was based on the following strain energy density $U$,

$$U = C_{10} \cdot (I_1 - 3) + C_{03} \cdot (I_2 - 3)^3 \tag{1}$$

where $I_1$ and $I_2$ are the first and the second invariants of the Cauchy-Green tensor, while the coefficients $C_{10}$ and $C_{03}$ are 0.019513 and 0.02976 MPa, respectively [14].

**2.1.2 Plaque model.** The plaque (Fig. 1) is modelled as a hollow cylinder (symmetric plaque) with a length of 3.68 mm, an internal diameter of 1.25 mm and a thickness of 0.45 mm. The plaque is discretised using 2560 8-node linear hybrid brick elements with a corresponding number of nodes of 3520, of which 920 are shared with the artery. A perfect bonding between the plaque and the arterial wall is considered. Similarly to the artery, a hyperelastic isotropic constitutive model is adopted with the following polynomial form:

$$U = C_{10} \cdot (I_1 - 3) + C_{02} \cdot (I_2 - 3)^2 + C_{03} \cdot (I_2 - 3)^3 \tag{2}$$

The values of the constants $C_{10}$, $C_{02}$ and $C_{03}$ are 0.04, 0.003 and 0.02976 MPa, respectively, as done similarly in [14]. They have been selected in order to simulate a calcified plaque, which is stiffer than the arterial wall.

**2.1.3 Stent model.** The stent design taken into consideration resembles that of a commercial intravascular stent (precisely, the CYPHER™ Sirolimus-eluting Coronary

Stent, Johnson & Johnson, Interventional System, Warren, NJ, USA). The main geometrical dimensions of the stent are: internal diameter of 0.9 mm, thickness of 0.14 mm and length of 3.68 mm. Only a single stent unit, *i.e*. an axial stent segment, is considered in the simulation (Fig 1).

This is a new generation stent whose design incorporates the presence of two different types of elements: *i*) tubular-like rings and *ii*) bridging members (links). The main function of the former is to maintain the vessel open after the stent expansion, while that of the latter is to link the rings in a flexible way during the delivery process. Hence, the former provide the stiffness whilst the latter determine the flexibility of the overall structure. To obtain the dimensions of the model a Cordis BX-Velocity (Johnson & Johnson, Interventional System, Warren, NJ, USA) stent is analyzed through the use of a Nikon SMZ800 stereo microscope (Nikon Corporation, Tokyo, Japan). The geometry of the model is created using the Rhinoceros 2.0 Evaluation CAD program (McNeel & Associates, Indianapolis, IN, USA). The stent is made of 316L stainless steel. The inelastic constitutive response is described through a Von Mises-Hill plasticity model. The Young modulus is 193 GPa, the Poisson ratio 0.3, the yield stress 205 MPa [11].

The yield stress is reduced to 105 MPa by using a kinematic hardening. Indeed, results from experimental tests carried out on real stent models showed a better agreement with the computational results when a reduction of the yield stress was considered [24]. The models are meshed with first-order interpolation shell elements. The number of elements was 2100.

The stent coating (thickness 5 μm) is not taken into account in the simulation of the stent expansion due to the fact that the polymer matrix does not influence the mechanical properties of the stent.

**2.1.4 Sensitivity Analysis.** A mesh sensitivity analysis was performed on both the vascular wall and the stent model. As regards the vascular wall four meshes with

increasing number of elements (4828, 9280, 12052 and 15808, respectively) were created. The Von Mises stresses in the vascular wall after the simulation of the stent expansion were different only with the coarsest mesh, while the others showed very similar results. The choice was for the mesh with 9280 elements (6720 for the artery and 2560 for the plaque). As regards the stent, shell elements were chosen after a comparison with a mesh made of 10-node tetrahedral elements in a free-expansion simulation. The pressure-diameter relationships were compared as in Migliavacca et al. [25]. Results of this sensitivity analysis at full stent expansion showed minimal differences, supporting the choice for the shell elements which are less demanding in terms of computational resources.

**2.1.5 Simulations and quantities of interest.** A large deformation analysis was performed using the ABAQUS commercial code. The nonlinear problem, due to material plasticity and contact constraint, was solved using a Newton-Raphson method. The convergence criterion here adopted consists of ensuring that the largest residual in the balance equations and the largest correction to any nodal unknown provided by the current Newton iteration are both smaller than a given tolerance. In particular, for the problem at hand the tolerance on the residual force was chosen as the 0.5% of the average force in the structure (averaged over space and time). Specific frictionless contact surfaces were introduced to model possible interactions between specific portions in the stent unit model with the artery and plaque. The contact constraint was defined by using the Lagrange multiplier approach, so that the constraint variable is the normal pressure and the constraint the surface penetration. In particular, we adopted the ABAQUS finite-sliding contact option, which allows for separation and sliding of finite amplitude, along with arbitrary rotation, between two 3D deformable body surfaces.

The outer cross sections of the artery were constrained in the longitudinal direction to simulate the fact that the considered model is not a stand-alone segment but is part of a

whole coronary artery. Furthermore, in an axial section located in the centre of the artery, three nodes forming the vertices of an equilateral triangle were constrained in the tangential direction to avoid the rotation of the structure. These conditions allowed the radial expansion of the artery. As regards the stent, we applied boundary conditions which constrain in the longitudinal and tangential directions three nodes forming the vertices of an equilateral triangle in the medial cross section of the stent itself.

A preliminary simulation on the artery was carried out in order to take into account an axial pretensioning of 5% [26]. As a result an axial stress state of 6 kPa was calculated, which was applied as initial stress state for the artery. A pressurization of the vascular wall (artery and plaque) of 100 mmHg was also applied. During this phase the diameter of the internal plaque increased from 1.25 mm to 1.46 mm and the diameter of the part of the artery without the stenosis from 2.15 mm to 3 mm. It corresponds to a stenosis of 76% in terms of area reduction in the central cross section. The deployment of the stent into the artery by balloon inflation was simulated in a simplified way. In particular, the balloon presence was discarded and the stent was expanded under displacement control up to a final diameter of 3 mm. This means that all the nodes of the stent were forced to have the same radial displacement. At this point the main quantities of interest, namely, the stresses (axial, radial and circumferential components) in the plaque and in the artery and the tissue prolapse (*tp*) between the stent struts were evaluated. Tissue prolapse is evaluated in absolute terms as the maximal protrusion of the plaque between the cells. A high value of tissue prolapse means a reduction of the free lumen and could be related to a low scaffolding capability of the stent.

### 2.2 Drug elution model

**2.2.1 The geometrical model for drug release simulations**. To create the computational model of the arterial wall for the mass transfer simulation, both the deformed artery and stent resulting from the stent expansion model were exported as a

point cloud and an appropriate tetrahedral finite element grid was generated using the mesh generator software Gambit (Gambit, Fluent Inc, Lebanon, NH, USA). Local grid refinement near the interface to the stent strut was applied to capture the expected high concentration variations (Fig. 2). The stent struts were assumed to be coated by a polymer matrix loaded with a medical drug and a topcoat film that separates the polymer matrix and the arterial wall. This film is aimed to slow down drug release into the arterial wall. A naive approach which applied to the present three dimensional geometry the numerical procedure used for two dimensions by Zunino [27], where the stent coating is modeled as a thin porous layer, turned out to be unaffordable at the computational level. Indeed the need to resolve the concentration in the extremely thin coating would drive an extremely and unnecessarily fine grid also in the rest of the computational domain, easily counting millions of tetrahedral elements for a single stent strut. A possibility to overcome this problem would be to use non conforming grids, which are however difficult to handle and prone to numerical errors. For this reasons and because of the geometrical complexity of the stent geometry, we chose not to consider the layers of the stent coating (polymer matrix and topcoat) as part of the three dimensional domain. Nevertheless, drug concentration was not assumed to be constant at the interface between the struts and the wall. Drug exchange between the stent and the wall was modelled by suitable transmission conditions described in section 2.2.3.

**2.2.2 A model for plasma filtration inside the artery.** The heterogeneous structure of the arterial wall ($\Omega_w$), which consists of randomly distributed fibres and cells, was mathematically treated on a macroscopic scale as a homogeneous porous medium [28], and the transport of the considered drug molecules was modelled by the macroscopic convection-diffusion equation. This framework has already been considered for the computer simulation of drug release [21, 29-32]. However, a well accepted model to describe these phenomena and achieve numerical simulations is not available yet. For

this reason, a detailed description of the specific features of the model is here reported.

In the governing equations for the mass transfer into the arterial walls, $\mathbf{u}_w$ denotes the volume averaged filtration velocity of the plasma (the liquid part of blood) into the wall. This filtration of blood plasma through the porous arterial wall layers is driven by the high pressure difference between the blood and the outer wall tissue [33]. Due to the small pore size of the wall layers, blood cells and the majority of macromolecules dissolved in the blood can not filtrate through the wall. This very slow process is governed by the Darcy's equation constrained with the solenoidal condition that ensures the mass conservation in the case of incompressible fluids. These equations, equipped with suitable boundary conditions read as follows,

$$\begin{aligned} \mathbf{u}_w &= -\frac{K_p}{\mu_p}\nabla p_w \qquad \text{in} \quad \Omega_{w.} \\ \nabla \cdot \mathbf{u}_w &= 0 \end{aligned} \tag{3}$$

In this formula, and also in the sequel, the operator nabla $\nabla = (\partial_x, \partial_y, \partial_z)$ in three dimensions, is used to represent the gradient ($\nabla p_w$) or the divergence ($\nabla \cdot \mathbf{u}_w$) of a scalar or vector function, respectively. Moreover, in equation (3), $K_p$=2·10$^{-14}$ cm$^2$ represents the Darcy's permeability of the media [34], while $\mu_p$=0.72·10$^{-2}$ g/(cm s) is the viscosity of plasma [35]. According to the Darcy's law, which depends only on the pressure gradient and not on the absolute value of the pressure, a difference of 70 mmHg [33] was imposed between the inner and the outer surface of the arterial wall by means of the boundary conditions. The pressure distribution, reported in figure 6, shows the pressure variations relative to a reference value of 760 mmHg. The corresponding pressure gradient induces a filtration velocity in the radial direction inside the wall.

**2.2.3 A pharmacokinetic model.** The drug release encompasses several processes that contribute to the transfer of the drug from the stent coating to the arterial walls. Some of these processes take place inside the coating, as for instance the dissolution of the drug,

some others take place inside the arterial walls, as diffusion, convection and binding with the extracellular matrix. Several models with very different level of complexity, are available to describe these phenomena, see for instance [36]. In this work, we picked out the models that turned out to be most effective to our study, according to simplicity and applicability criteria.

For the dynamics of the drug inside the arterial walls, the quantity of interest was the volume averaged mass concentration ($c_w$). Being interested in addressing the drug interactions with the tissue, two possible states of a drug into the arterial wall were taken into account: *i*) the drug that is dissolved into the plasma, addressed in the following as the 'free' drug and denoted with $c_{w,f}$ and *ii*) the drug that is bound to specific receptors of the extracellular matrix of the tissue, addressed as the 'bound' drug and indicated by $c_{w,b}$. Then, the volume averaged concentration corresponded point-wise as the sum of these two quantities. According to the models proposed in Creel et al. [29], the concentration of the free drug was related to the total concentration by a constant factor; in particular $c_{w,f} = c_w/k_w$ where $k_w$ is the so called partition coefficient that defines the ratio of drug bound to the tissue with respect to the drug dissolved in the fluid, under the assumption of equilibrium between the two states of the drug. More precisely, Creel et al. [29] reported that several arterial samples were incubated in paclitaxel solutions at different bulk concentrations ($c_{w,f}$ ) for 72 hours, which was assumed to be enough to reach the equilibrium of the binding process. Then, the tissue concentration ($c_w$) was measured and related to the bulk concentration in order to quantify $k_w = c_w/c_{w,f}$. Although this ratio is not independent of the bulk concentration, we consider the average value $k_w=20$.

The governing equation for the concentration of the drug inside the arterial walls then reads

$$\frac{\partial c_w}{\partial t} + \frac{\gamma_w}{k_w}\mathbf{u}_w \nabla c_w - D_w \Delta c_w = 0 \quad \text{in} \quad \Omega_w \tag{4}$$

where $D_w$ is the effective diffusion coefficient of the drug in the porous wall. Equation (4) accounts for the convective transport field of the plasma inside the wall, driven by the filtration velocity $\mathbf{u}_w$. The hindrance coefficient $\gamma_w$ accounts for the decrease of convective transport due to collisions of the transported particles with the structure of the porous wall ( $0 < \gamma_w \leq 1$).

The partial differential equation (4) has to be provided with appropriate boundary conditions. The boundary of the arterial wall segment can be divided in the following parts: the interface to the coated stent struts, the interface to the arterial lumen, the interface to the adventitia and the artificial cutting interfaces at the beginning and the end of the arterial segment (Fig. 3).

Zero concentration was assumed at the interface to the lumen, that is

$$c_w = 0 \quad \text{on} \quad \Gamma_b \tag{5}$$

This boundary condition arises from the assumption that the concentration at the interface equals the concentration of the drug in the blood, which is negligible. The cutting interfaces ($\Gamma_c$) are assumed to be sufficiently far away from the domain of interest (stent). Also on these boundaries a zero concentration is assumed, i.e.

$$c_w = 0 \quad \text{on} \quad \Gamma_c \tag{6}$$

At the outer boundary of the arterial wall ($\Gamma_a$) the continuity of the diffusive fluxes was assumed and the boundary was modelled as a membrane, leading to

$$-D_w \frac{\partial c_w}{\partial \mathbf{n}_w} = P_V \left( \frac{c_w}{\varepsilon_w k_w} \right) \quad \text{on} \quad \Gamma_a \tag{7}$$

where the permeability is denoted by $P_V$ and $\varepsilon_w$ is the porosity of the wall. The outward oriented normal vector on the wall is indicated by $\mathbf{n}_w$.

Concerning the phenomena that take place inside the stent coating, we considered first of all the drug dissolution that is mainly the interaction of the solid drug with the surrounding fluid, which in our case is the blood plasma. After the dissolution process,

the drug is able to diffuse freely inside the surrounding medium. We observed that in our case the surrounding medium was the porous medium that describes the stent coating and not a free fluid, as prescribed by the classical theory. For this reason, we assumed that the diffusion process after the dissolution was much slower than the dissolution itself. As a consequence of that, we have neglectd the dissolution process in our description of drug release from the stent coating to the arterial walls. By consequence, we have denoted by $c_c$ the volume averaged concentration of the drug dissolved into the stent coating. The drug release from the stent to the wall was described by means of appropriate transmission conditions at the interface ($\Gamma_s$) between the struts and the arterial wall (see Fig. 3). These conditions provided the transient drug flux at the interface between the stent coating and the wall. The transmission condition at the interface with the coated stent struts was derived by means of the Fick's law,

$$J_S = D_w \frac{\partial c_w}{\partial \mathbf{n}_w} \quad \text{on} \quad \Gamma_s \tag{8}$$

The flux of drug from the stent coating to the interface is $J_S$ and the right hand side of equation (8) denotes the diffusive flux into the arterial wall. This flux was approximated by an analytical equation which acts on each finite element wall node located at the interface with the coating. It fulfils mass conservation, that means that the rate of change of the drug stored in the coating $M_c$ is given by the flux through the interface:

$$\frac{\partial}{\partial t} M_c = -\int_{\Gamma_s} J_S \, d\Gamma \tag{9}$$

The value of the flux can be approximated by means of an electrical analogy [22]. For the polymer matrix characterized by a thickness $\Delta l$, and a diffusion coefficient $D_c$ and the topcoat characterized by a permeability coefficient $P$ we had

$$J_S = \frac{D_c}{\Delta l \theta(t)} \left( c_{c,2} - c_{c,1} \right) = P \left( \frac{c_{c,1}}{k_c \varepsilon_c} - \frac{c_w}{k_w \varepsilon_w} \right) \tag{10}$$

where ($c_{c,2}$-$c_{c,1}$) denotes the concentration drop in the polymer matrix and $c_w$ is the wall

concentration at the interface. $\theta(t)$ denotes a time dependent correction term of the coating resistance due to the occurrence of a concentration boundary layer. This correction was derived from the mathematical theory of the heat equation [37]. Using the approximation

$$M_c = \int_{\Gamma_s} \tilde{M}_c d\Gamma \approx \int_{\Gamma_s} 1/2\left(c_{c,1} + c_{c,2}\right) d\Gamma \tag{11}$$

in equation (9) the integration over $\Gamma_s$ can be eliminated. Substituting the result into equation (10) the desired analytical expression of $M_c$ and $J_S$ in terms of the layer parameters was then obtained.

Although the drug in combination with the CYPHER$^{TM}$ stent is sirolimus the parameters used for the model correspond to the hydrophobic drug paclitaxel (taxus), which has a similar molecular weight (Hose et al. [21]). The values of the parameters were taken from Creel et al. [29] and Hwang et al. [31]. The diffusion coefficient of taxus in the polymer matrix is $D_c$=1.0·10$^{-11}$ cm$^2$/s and in the arterial wall $D_w$=2.2·10$^{-9}$ cm$^2$/s. The permeability coefficient of the topcoat is $P$=1.0·10$^{-8}$ cm/s. The constant thickness of the coating is $\Delta l$=5μm. The porosities of the polymer matrix and the wall are $\varepsilon_c$=0.1 and $\varepsilon_w$=0.61. The hindrance coefficient is $\gamma_w$=1.0. Taxus is a highly hydrophobic drug resulting in a large partition coefficient in the arterial wall $k_w$=20.0. The partition coefficient in the polymer matrix is $k_c$=1.0 since there are no binding effects between the polymer and the drug. The permeability applied to the interface between the arterial wall and the vasa vasorum is $P_V$=1.0·10$^{-4}$ cm/s. The initial values of the drug concentration in the coating and wall are $c_c^0/C_0 \equiv 1.0$ and $c_w^0/C_0 \equiv 0.0$.

**2.2.4 Sensitivity analysis.** A mesh sensitivity analysis was performed by increasing the number of elements by 50% over the previous mesh. Due to the high computational cost the simulation with the refined grid was carried out for a release period of one day instead of the time interval of 6 day foreseen for the numerical study. The results were

compared by calculating the relative approximation error

$$E(t) = \frac{\int_{\Omega_w} |c_H(x,t) - c_h(x,t)| dx}{\int_{\Omega_w} | c_h(x,t) | dx} \quad (12)$$

for each time step, where $c_H(x,t)$ and $c_h(x,t)$ denote the concentration approximation on the original finite element mesh and on the refined mesh respectively. The maximal value of the relative approximation error, $E(t)$, was 3% and it occured after 19 hours. This result demonstrated that it was not essential to refine the original mesh to approximate the concentration of the drug in the arterial walls.

**2.2.5 Simulations and quantities of interest.** The numerical solution of the partial differential equations describing the plasma filtration and the mass transport in the arterial wall was based on the finite element Galerkin method, which requires the translation of the equations into appropriate variational forms that are solved in finite element subspaces [35,38]. The discretization of the time derivatives used backward finite differences (implicit Euler scheme). In particular, Darcy's equations (3) was discretised by means of Raviart-Thomas zeroth order elements, while the governing equations for drug release, from (4) to (11), was approximated with linear Lagrangian conforming elements.

The output of the numerical simulations of drug release consisted in the pressure field, relative to the pressure in the adventitia, the filtration velocity of plasma and the drug concentration. The pressure was piecewise constant in each element of the computational mesh, while the velocity and the concentration were calculated at each node of the mesh and interpolated at any point in between them.

In order to analyse the efficacy of drug release it was useful to manipulate these quantities in a postprocessing step. A significant parameter for the therapeutic effect of the released drug is the drug dose that is the accumulative concentration integrated over

time along the interval of interest. Furthermore, the drug residence time at each location inside the wall was considered. Given the absolute maximal concentration $C_{max}$ = max $c(t,x)$, the residence times $T_{10\%}(x)$ and $T_{1\%}(x)$ were defined as the total amount of time that a concentration higher than 10% or 1% of $C_{max}$, respectively, resides at a fixed location x inside the wall. Finally, the dynamics over time of the drug release process from the stent to the wall was quantified. For this purpose, two indicators were introduced: the amount of drug cast in the stent at any time after the stent implantation (denoted with $M_{stent}(t)$) and the amount of drug that was released into the wall at any time after the stent implantation (denoted with $M_{wall}(t)$). Both quantities were normalized with respect to the total amount of drug

## 3. Results

### *3.1 Stent expansion model*

Results in terms of radial, circumferential and axial stresses in the artery and plaque are reported in Fig. 4. The stresses are generally higher in the plaque than in the artery. In particular, a difference of one order of magnitude is observed. The magnitude of the radial and circumferential stresses in the plaque is quite similar, while is lower in the axial direction. Furthermore, it is possible to observe the 'imprints' of the stent struts on the vascular wall. The highest compressive stresses in the radial direction are located in the areas of contact between the stent struts and the plaque. The circumferential stresses show a considerable gradient from the internal to the external part of the arterial wall: the tensile stresses are maximal between the stent struts where tissue prolapse is present. Figure 5 reports the radial displacements in the cross sections of the vessel. The tissue prolapse (*tp)* is clearly visible. The numerical values of *tp* is 0.05 mm.

### *3.2 Drug elution model*

Figure 6 (left) shows the pressure distribution in the arterial wall, relative to the pressure

in the adventita. A constant pressure difference of 70 mmHg between lumen and adventitia was assumed in the calculation. The corresponding value of the filtration velocity is in the range of $10^{-6}$ cm/s, which is in good agreement with measured values [33]. The value of the filtration depends strongly on the wall thickness and is about 2 times lower in the region of the plaque. The main direction of the flow is normal to the wall in direction to the adventitia, it is slightly disturbed near the region of the stent struts (Fig. 6, right).

Figure 7 (panel a) depicts the concentration isolines of taxus on a cylindrical surface inside the wall at selected times. The average distance of the cylinder from the endothelium is 0.25 mm which corresponds to 25% of the wall thickness in the stenosed region. It can be seen that in the early release phase the drug concentration is highly dependent on the design of the stent struts. After some days the drug spreads more uniformly inside the wall (Fig. 7, panel a - bottom). The concentration of the drug decreases relatively fast and nearly no drug is left in the arterial wall at the end of the simulation period of six days (consider the different scale of the concentration in Fig. 7). Figure 7 (panel c) reports the drug dose inside the arterial wall. It shows that the drug dose and therewith the efficacy of the stent strongly depends on its geometry even if after some days a relatively uniform drug distribution in the wall can be demonstrated (Fig. 7, panel a - bottom). The dependence on the stent geometry of the drug efficacy inside the arterial wall is confirmed by the analysis of the residence time at each location inside the wall. The surface plots of $T_{10\%}(x)$ and $T_{1\%}(x)$ on the cylindrical reference surface inside the wall are reported in Fig. 7 (panel b).

Finally, Fig. 8 shows the total amount of drug stored in the stent coating ($M_{\text{stent}}(t)$) and in the arterial wall ($M_{\text{wall}}(t)$) for a period of 6 days after the implantation. The amount of drug in the wall reaches the maximal value of 65% of the drug initially loaded in the coating after 10 hours. First of all, these data suggest that, in average, the drug release process is relatively fast in this stent configuration. Indeed, after 1 day less than 10% of

the initial drug load is left in the stent coating. This value decreases to 2% after 6 days. Furthermore, the peak value of the amount of drug inside the wall is quite high. This is in part motivated by the fact that in the simulation it is assumed that only the contact surface between the stent struts and the wall is coated. For this reason the drug can be only released into the arterial wall (Fig. 3, right) and no direct interaction between the drug and the blood is possible. The average residence time $T_{10\%}$, which is defined as a time when the amount of drug within the vessel dropped down to 10% with respect to the peak value, is 83 hours. This means that, on average, a non negligible amount of drug is present in the wall although the drug distribution is not uniform.

## 4 Discussion

This study presents an approach to simulate the interaction of a coronary stent with the vascular wall and the elution of the drug within the arterial wall.

Although works on mechanical behaviour of stents [39,40] and their interaction with arterial wall [13-17] are present in the literature, to our knowledge, this study is the first to investigate the drug elution after the simulation of a stent expansion.

Looking at the structural part, from analyses like those carried out in this study, it is possible to give a clue of the stress field generated by the stent expansion and detect the most stressed vascular areas, which are in correspondence of the contact with the stent struts. It is also possible to observe the differences in the mechanical stress state between the atherosclerotic plaque and the arterial wall. Furthermore, tissue protrusion within the stent struts, which reveals the stent scaffold properties, can be quantified, too. However, it is difficult, for example, to find a strict correlation between the geometrical design (such as the stent thickness or the length of the links), the tissue prolapse and the in-stent restenosis, unless these data are complemented with those obtained from clinical trials aimed at comparing the influence of the stent design on the degree of restenosis. For this purpose, different stent designs should be analysed and compared in

terms of mechanical quantities generated in the vascular wall; results from the computations should be correlated with the clinical data from purposely designed clinical follow-ups. Caution should be adopted if the results from the simulations are compared with clinical trials already present in the literature; they often refer only to two different stent designs and, even for the same stent design, sometimes they adopt a different methodology in the design of the study (*i.e.* patient recruitment, primary or secondary endpoints) [41-43].

In the present model homogenous material properties were assumed for both the arterial wall and the atherosclerotic plaque. Holzapfel and colleagues [26] have recently reported tensile test data from 13 non-stenotic human left anterior descending coronary arteries where the stress-stretch responses for the individual tissues (intima, media and adventitia) showed pronounced mechanical heterogeneity. We cannot distinguish in our model among the three arterial layers; however, the stress-stretch curve adopted here is situated in the range observed in the experiments by Holzapfel et al. [26]. The circumferential pretensioning of the arterial wall has not been taken into consideration in our models.

A further limitation of the present study is the application of displacement boundary conditions to simulate the stent expansion. Indeed, a proper description of the stenting procedure should include the modelling of the balloon inflation and deflation as well as the implementation of a proper constitutive model to describe plaque response up to fracture. However this is beyond the scope of this work. In fact, in this work we are interested in the stress and strain fields the stent produces on the atherosclerotic walls at its final configuration reached by imposing a radial displacement to all the nodes of the stent to simulate the inflation of the balloon.

Lastly, we believe that the effects of the vessel curvature as well as those of the actual stent length (different from that of a single unit as investigated in this study) could be important issues towards a full understanding of this interventional procedure.

However, in previous studies of ours we verified that the stent length does not add information on the flexibility properties of the stents with respect to the results obtained from the expansion of the single stent unit [44]. Nonetheless, this methodology, although still simplified, could be highly beneficial to compare different stent designs. Future research will be devoted to removing the above limitations so as to achieve a more realistic description of the stenting procedure.

As regards the drug release from drug eluting stents, several studies have been carried out in the literature with different complexity at the modelling and the computational level. For instance Hwang et al. [31] considered a basic model in two space dimensions for convection and diffusion of the drug into the arterial wall in order to investigate the role of convection with respect to the drug distribution inside the wall. This study has later been improved on the modelling side by Zunino [27], by introducing the presence of the stent coating and the topcoat in the case of a very simple geometrical model, and also by Hose et al. [21] who studied the drug release in the arterial wall in three space dimensions. However, the geometrical model considered in those previous works is not fully realistic because it does not take into account the geometrical coupling between the stent and the arterial wall, which is indeed one of the focuses of the present study. The various parameters governing the transport and diffusion of the drug under study have been taken from the available literature. The results obtained look qualitatively correct and give confidence on the capability of the model to correctly describe the elution process. However, specially designed in-vitro experimentation is required to have a quantitative validation of the tranport model and possibly better assess the transport parameters. Work in this direction is currently under way.

Starting from the realistic arterial geometry provided by the mechanical analysis of the stent expansion, the drug elution process has been simulated. The numerical investigation of the drug elution represents a valuable tool to collect quantitative information about the efficacy of the drug inside the arterial wall. Indeed, the

visualization of extensive data as the drug concentration, the dose and the residence time could provide a better insight for the evaluation and the understanding of the benefit that drug eluting stents bring to the treatment of coronary diseases. For instance, the analysis of these quantities suggests that the coating configuration considered here provides a relatively fast release. Furthermore, the distribution of the drug inside the wall is not uniform and it is strongly influenced by the geometry of the struts. For this reason, from the point of view of drug delivery, a different geometrical design of the stent could be envisaged. For this kind of investigations, numerical simulations represent a powerful opportunity to improve the technology behind drug eluting stents. Indeed, numerical studies allow to explore several configurations concerning the materials constituting the stent coating and the geometrical design of the stent.

The mathematical models for the drug elution presented here feature some limitations that may affect the results form a merely quantitative point of view.

For example, since this work addresses three-dimensional simulations on complex realistic geometries that require high computational efforts, it was not possible to consider the blood fluid dynamics inside the arterial lumen. This choice precluded the possibility to analyse the effect of flow-mediated deposition of the blood-solubilized drug, which, according to Balakrishnan et al. [32], seems to have a relevant influence on the distribution of the drug into the arterial walls. Moreover, the present study does not consider the transient and reversible binding process between the drug and the extracellular matrix, mainly constituted by elastin, collagen fibers and proteoglycans. A model for such phenomena was proposed by Sakharov et. al [45], where numerical simulations of drug release in a simplified geometrical setting were provided as well, putting into evidence the beneficial role of binding effects to prolong the presence of the drug in the target tissue. A similar model can be introduced in our methodology for drug release with minor changes with respect to the present setting. This study will be considered in a forthcoming paper. A further improvement of the present work may

consider the influence of the deformation state of the extracellular matrix on the transport properties of water and drug inside the wall, which are characterized by the permeability of the wall layers (endothelium, intima and media). This dependence has been put into evidence by means of experimental studies reported in Winlove et al. [46] and in Weinberg et al. [47]. However, this development seems to be a demanding challenge since a precise mathematical model to describe these phenomena is still missing.

## ACKNOWLEDGEMENTS

*This work has been supported by Fondazione Cariplo, Milan, Italy, under the project "Modellistica Matematica di Materiali Microstrutturati per Dispositivi a Rilascio di Farmaco". Partial support from the European Community´s Human Potential Programme under contract HPRN-CT-2002-00270 Haemodel is acknowledged, too.*

## REFERENCES

[1] Serruys, P.W., de Jaegere, P., Kiemeneij, F., Macaya, C., Rutsch, W., Heyndrickx, G., Emanuelsson, H., Marco, J., Legrand, V., Materne, P., Belardi, J., Sigwart, U., Colombo, A., Goy, J.J., van den Heuvel, P., Delcan, J., Morel, M.-A., 1994, A comparison of balloon-expandable-stent implantation with balloon angioplasty in patients with coronary artery disease. Benestent Study Group. *The New England Journal of Medicine*, **331**, 489-495.

[2] Fischman, D.L., Leon, M.B., Baim, D.S., Schatz, R.A., Savage, M.P., Penn, I., Detre, K., Veltri, L., Ricci, D., Nobuyoshi, M., Cleman, M., Heuser, R., Almond, D., Teirstein, P.S., Fish, R.D., Colombo, A., Brinker, J., Moses, J., Shaknovich, A., Hirshfeld, J., Bailey, S., Ellis, S., Rake, R., Goldberg, S., 1994, A randomized comparison of coronary-stent placement and balloon angioplasty in the treatment of coronary artery disease. Stent Restenosis Study Investigators. *The New England Journal of Medicine*, **331**, 496-501.

[3] Serruys, P.W., Luijten, H.E., Beatt, K.J., Geuskens, R., de Feyter, P.J., van den Brand, M., Reiber, J.H., ten Katen, H.J., van Es, G.A., Hugenholtz, P.G., 1998, Incidence of restenosis after successful coronary angioplasty: a time-related phenomenon: a quantitative angiographic study in 342 consecutive patients at 1, 2, 3, and 4 months. *Circulation*, **77**, 361-371.

[4] Edelman, E.R., Rogers C., 1998, Pathobiologic responses to stenting. *The American Journal of Cardiology*, **81**(7A), 4E-6E.

[5] Schwartz, R.S., Huber, K.C., Murphy, J.G., Edwards, W.D., Camrud, A.R., Vlietstra, R.E., Holmes, D.R., 1992, Restenosis and the proportional neointimal response to coronary artery injury: results in a porcine model. *Journal of the American Coillege of Cardiology*, **19**, 267-274.

[6] Kornowski, R., Hong, M.K., Tio, F.O., Bramwell, O., Wu, H., Leon, M.B., 1998, In-

stent restenosis: contributions of inflammatory responses and arterial injury to neointimal hyperplasia. *Journal of the American Coillege of Cardiology*, **31**, 224-230.

[7] Grenacher L, Rohde S, Ganger E, Deutsch J, Kauffmann GW, Richter GM., 2006, In Vitro Comparison of Self-Expanding Versus Balloon-Expandable Stents in a Human Ex Vivo Model. *Cardiovascular and Interventional Radiology*, **29**, 249-254.

[8] Rogers, C., Edelman, E.R., 1995, Endovascular stent design dictates experimental restenosis and trombosis. *Circulation*, **91**, 2995-3001.

[9] Sanmartin M, Goicolea J, Garcia C, Garcia J, Crespo A, Rodriguez J, Goicolea JM., 2006, Influence of Shear Stress on In-Stent Restenosis: In Vivo Study Using 3D Reconstruction and Computational Fluid Dynamics. *Revista Española de Cardiología*, **59**, 20-27.

[10] Wentzel, J.J., Krams, R., Schuurbiers, J.C., Oomen, J.A., Kloet, J., van Der Giessen, W.J., Serruys, P.W., Slager, C.J., 2001, Relationship between neointimal thickness and shear stress after Wallstent implantation in human coronary arteries. *Circulation*, **103**, 1740-1745.

[11] Auricchio, F., Di Loreto, M., Sacco, E., 2001, Finite-element analysis of a stenotic artery revascularization through a stent insertion. *Computer Methods in Biomechanics and Biomedical Engineering*, **4**, 249-263.

[12] Holzapfel, G.A., Stadler, M., Schulze-Bauer, C.A.J., 2002, A layer-specific three-dimensional model for the simulation of balloon angioplasty using magnetic resonance imaging and mechanical testing. *Annals of Biomedical Engineering*, **30**, 753-767.

[13] Prendergast, P.J., Lally, C., Daly, S., Reid, A.J., Lee, T.C., Quinn, D., Dolan, F., 2003, Analysis of prolapse in cardiovascular stents: a constitutive equation for vascular tissue and finite-element modelling. *Journal of Biomechanical Engineering*, **125**, 692-699.

[14] Migliavacca, F., Petrini, L., Massarotti, P., Schievano, S., Auricchio, F., Dubini, G., 2004, Stainless and shape memory alloy coronary stents: a computational study on the interaction with the vascular wall. *Biomechanics and Modeling in Mechanobiology*, **2**, 205-217.

[15] Lally, C., Dolan, F., Prendergast, P.J., 2005, Cardiovascular stent design and vessel stresses: a finite element analysis. *Journal of Biomechanics*, **38**, 1574-1581.

[16] Holzapfel, G.A., Stadler, M., Gasser, T. C., 2005, Changes in the mechanical environment of stenotic arteries during interaction with stents: computational assessment of parametric stent designs. *Journal of Biomechanical Engineering*, **127**, 166-180.

[17] Liang, D.K., Yang, D.Z., Qi, M., Wang, W.Q., 2005, Finite element analysis of the implantation of a balloon-expandable stent in a stenosed artery. *International Journal of Cardiology*, **104**, 314-318.

[18] Saia, F., Marzocchi, A., Serruys, P.W., 2005, Drug-eluting stents. The third revolution in percutaneous coronary intervention. *Italian Heart Journal*, **6**, 289-303.

[19] Moses, J.W., Leon, M.B., Popma, J.J., Fitzgerald, P.J., Holmes, D.R., O'Shaughnessy, C., Caputo, R.P., Kereiakes, D.J., Williams, D.O., Teirstein, P.S., Jaeger, J.L., Kuntz, R.E., 2003, SIRIUS Investigators: Sirolimus-eluting stents versus standard stents in patients with stenosis in a native coronary artery. *The New England Journal of Medicine*, **349**, 1315-1323.

[20] Morice, M.C., Serruys, P.W., Sousa, J.E., Fajadet, J., Ban Hayashi, E., Perin, M., Colombo, A., Schuler, G., Barragan, P., Guagliumi, G., Molnar, F., Falotico, R., 2002, A randomized comparison of a sirolimus-eluting stent with a standard stent for coronary revascularization. *The New England Journal of Medicine*, **346**, 1773-1780.

[21] Hose, D.R., Narracott, A.J., Griffiths, B., Mahmood, S., Gunn, J., Sweeney, D.,

Lawford, P.V., 2004, A thermal analogy for modelling drug elution from cardiovascular stents. *Computer Methods in Biomechanics and Biomedical Engineering*, **7**, 257-264.

[22] Prosi, M., Zunino, P., Perktold, K., Quarteroni, A., 2005, Mathematical and numerical models for transfer of low-density lipoproteins through the arterial walls: a new methodology for the model set up with applications to the study of disturbed lumenal flow. *Journal of Biomechanics*, **38**, 903-917.

[23] Hayashi, K., Imai, Y., 1997, Tensile property of atheromatous plaque and an analysis of stress in atherosclerotic wall. *Journal of Biomechanics*, **30**, 573-579.

[24] Migliavacca, F., Petrini, L., Montanari, V., Quagliana, I., Auricchio, F., Dubini, G., 2005, A predictive study of the mechanical behaviour of coronary stents by computer modelling. *Medical Engineering & Physics*, **27**, 13-18.

[25] Migliavacca, F., Petrini, L., Colombo, M., Auricchio, F., Pietrabissa, R., 2002, Mechanical behavior of coronary stents investigated through the finite element method. *Journal of Biomechanics*, **35**, 803-811.

[26] Holzapfel, G.A., Sommer, G., Gasser, C., Regitnig, P., 2005, Determination of the layer-specific mechanical properties of human coronary arteries with intimal thickening, and related constitutive modelling. *American Journal of Physiology. Heart and Circulatory Physiology*, **289**, H2048-H2058.

[27] Zunino, P., 2004, Multidimensional pharmacokinetic models applied to the design of drug-eluting stents. *Int. Jour. of Cardiovascular Engineering*, **4**, 181-191.

[28] Shyy, W., Thakur, S., Ouyang, H., Liu, J., Blosch, E., 1997, *Computational Techniques for Complex Transport Phenomena* (Cambridge University Press, UK)

[29] Creel, C.J., Lovich, M.A., Edelman, E.R., 2000, Arterial palcitaxel distribution and deposition. *Circulation Research*, **86**, 879-884.

[30] Delfour, M.C. Garon, A., Longo, V., 2005, Modeling and design of coated stents to

optimize the effect of the dose. *SIAM Journal on Applied Mathematics*, **65**, 858-881.

[31] Hwang, C.W., Wu, D., Edelman, E.R., 2001, Physiological transport forces govern drug distribution for stent based delivery. *Circulation*, **204**, 600-605..

[32] Balakrishnan, B., Tzafriri, A.R., Seifert, P., Groothuis, A., Rogers, C., Edelman E.R., 2005, Strut Position, Blood Flow, and Drug Deposition. Implications for Single and Overlapping Drug-Eluting Stents. *Circulation*, **111**, 2958-2965.

[33] Meyer, G., Merval, R., Tedgui, A., (1996), Effects of pressure stretch and convection on low-density lipoprotein and albumin uptake in the rabbit aortic wall. *Circulation Research*, **79**, 532-540.

[34] Whale, M., Grodzisky, A., Johnson, M., 1996, The effect of aging and pressure on the specific hydraulic conductivity of the aortic wall. *Biorheology*, **33**, 17-44.

[35] Karner, G., Perktold, K., Zehentner, H.P., Prosi, M., 2000, Mass transport in large arteries and through the arterial wall, In: Verdonk, P., Perktold, K., (Eds.), Intra and Extracorporeal Cardiovascular Fluid Dynamics. WIT-Press Computational Mechanics Publications, Southampton, Boston, pp. 209-247.

[36] Macheras, P., Iliadis, A., 2006, *Modeling in Biopharmaceutics, Pharmacokinetics, and Pharmacodynamics. Homogeneous and Heterogeneous approaches*, (Springer).

[37] Bird, R.B., Lightfoot, E.N., Stewart, W.E., 2001, *Transport Phenomena*, 2nd Edition, (John Wiley & Sons).

[38] Zunino, P., 2002, Mathematical and numerical modeling of mass transfer in the vascular system. PhD. Thesis, Ecole Polythechnique Federale de Lausanne, Lausanne.

[39] Wang WQ, Liang DK, Yang DZ, Qi M., 2006, Analysis of the transient expansion behavior and design optimization of coronary stents by finite element method. *Journal of Biomechanics*, **39**, 21-32.

[40] Theriault P, Terriault P, Brailovski V, Gallo R., 2005, Finite element modeling of a progressively expanding shape memory stent. *Journal of Biomechanics*, 2005 Oct 28;

[41] Pache, J., Kastrati, A., Mehilli, J., Schuhlen, H., Dotzer, F., Hausleiter, J., Fleckenstein, M., Neumann, F.J., Sattelberger, U., Schmitt, C., Muller, M., Dirschinger, J., Schomig, A., 2003, Intracoronary stenting and angiographic results: strut thickness effect on restenosis outcome (ISAR-STEREO-2) trial. *Journal of the American College of Cardiology*. **41**, 1283-1288.

[42] Morice, M.C., Colombo, A., Meier, B., Serruys, P., Tamburino, C., Guagliumi, G., Sousa, E., Stoll, H.P., 2006, Sirolimus- vs paclitaxel-eluting stents in de novo coronary artery lesions: the REALITY trial: a randomized controlled trial. *JAMA : the journal of the American Medical Association*, **295**, 895-904.

[43] Mehilli, J., Dibra, A., Kastrati, A., Pache, J., Dirschinger, J., Schomig, A., 2006, Randomized trial of paclitaxel- and sirolimus-eluting stents in small coronary vessels. *European Heart Journal*, **27**, 260-266.

[44] Petrini, L., Migliavacca, F., Auricchio, F., Dubini, G., 2002, Numerical investigation of the intravascular coronary stent flexibility. *Journal of Biomechanics*, **37**, 495-501.

[45] Sakharov, D.V., Kalache, L.V., Rijken, D.C., 2002, Numerical simulation of local pharmacokinetics of a drug after intravascular delivery with an eluting stent. *Journal of Drug Targeting*, **10**, 507-513.

[46] Winlove, C.P., Parker, K.H., 1993, Vascular biophysics: mechanics and permeability. *European Respiratory Review*, **16**, 535-542.

[47] Weinberg, P.D., Winlove, C.P., Parker, K.H., 1995, The distribution of water in arterial elastin: effects of mechanical stress, osmotic pressure and temperature. *Biopolymers*, **35**, 161-169.

**LEGENDS**

Figure 1: 3-D model of the atherosclerotic coronary artery and the stent: open view of the whole model (top). Mesh of half model of the vessel (bottom left) and of the stent (right bottom).

Figure 2: Expanded geometric model of the arterial wall with the discretization used for the simulation of the drug elution.

Figure 3: Schematic illustration of the geometric model with indication of the different domains and boundaries. The drug is released from the interface $\Gamma_s$ (interface between stent coating and arterial wall) in direction of the arterial wall. $\Gamma_{a,}$ $\Gamma_b$ and $\Gamma_c$ are the outer boundary of the arterial wall, the interface between the arterial wall and the blood and the cutting interfaces, respectively.

Figure 4: Radial, circumferential and axial stresses in the artery (top) and the plaque (bottom). Legends for the three stress components in the plaque are different.

Figure 5: Color contour maps of the radial displacements in half model (left) and in the central cross section of the model (right). The measurements report the minimum inner radius reached after the expansion of the stent to a final diameter of 3 mm. The tissue prolapse (0.05 mm) is computable from this map.

Figure 6: Figure 6: Pressure distribution in the arterial wall (left) and vector field in the region of a stent strut (right - the contact area is indicated by a black line). The results were obtained by applying a pressure difference of 70 mmHg between inner and outer wall surface, around a reference value of 760 mmHg.

Figure 7: Wall concentration distribution on a cylinder (panel a) after 10 hours (left, top), 1 day (right, top), 3days (left, bottom), 6 days(right, bottom). Local residence time in days defined by the period in which the local concentration is higher than 10% ($T_{10\%}$, left) or 1% ($T_{1\%}$, right) of the maximal concentration in the wall (panal b). Dose distribution of taxus on a cylinder in the arterial wall after 6 days (panel c).

Figure 8: Drug release dynamics - amount of drug stored in the stent coating ($M_{stent}(t)$) and in the arterial wall ($M_{wall}(t)$) for a period of 6 days after the implantation.

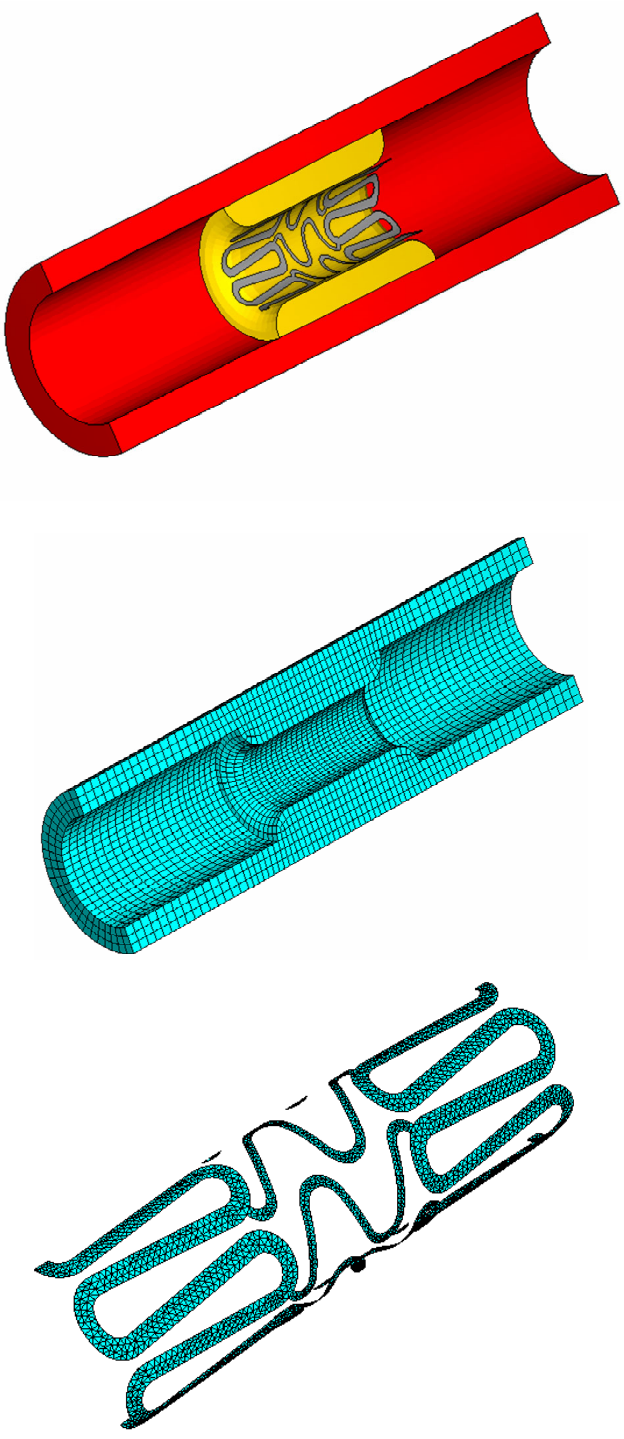

Figure 1

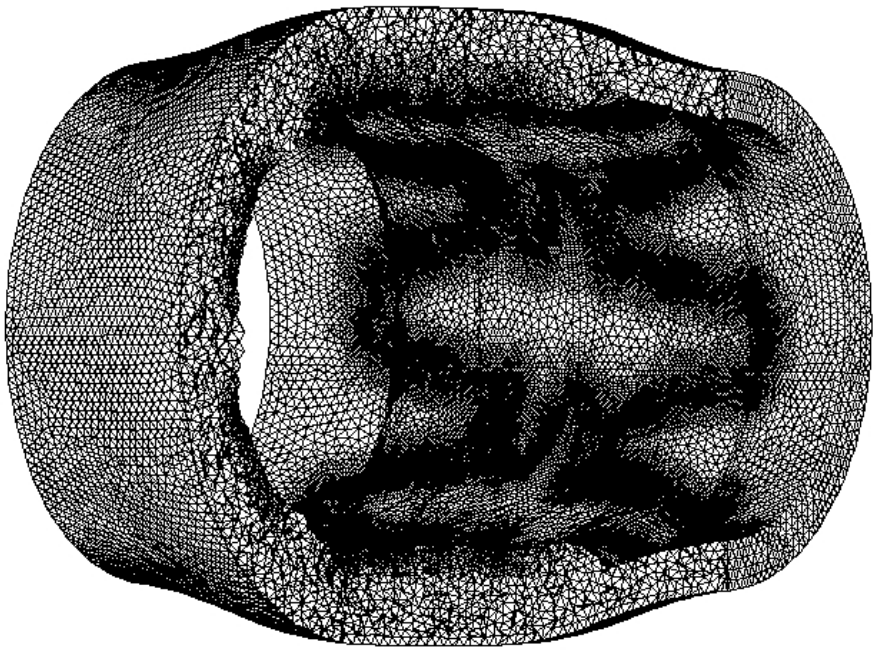

Figure 2

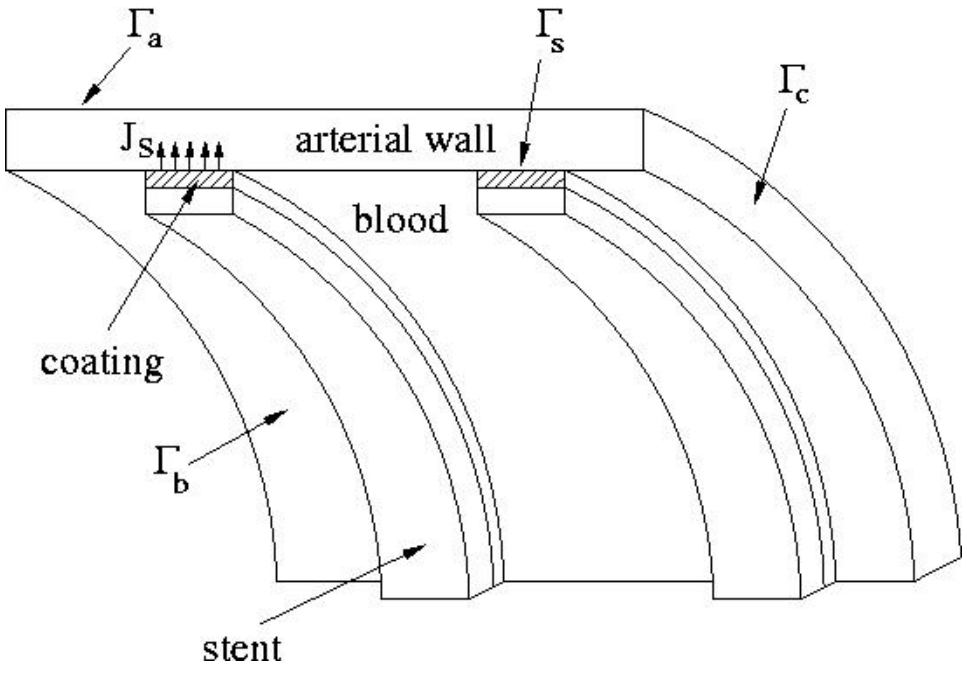


Figure 3

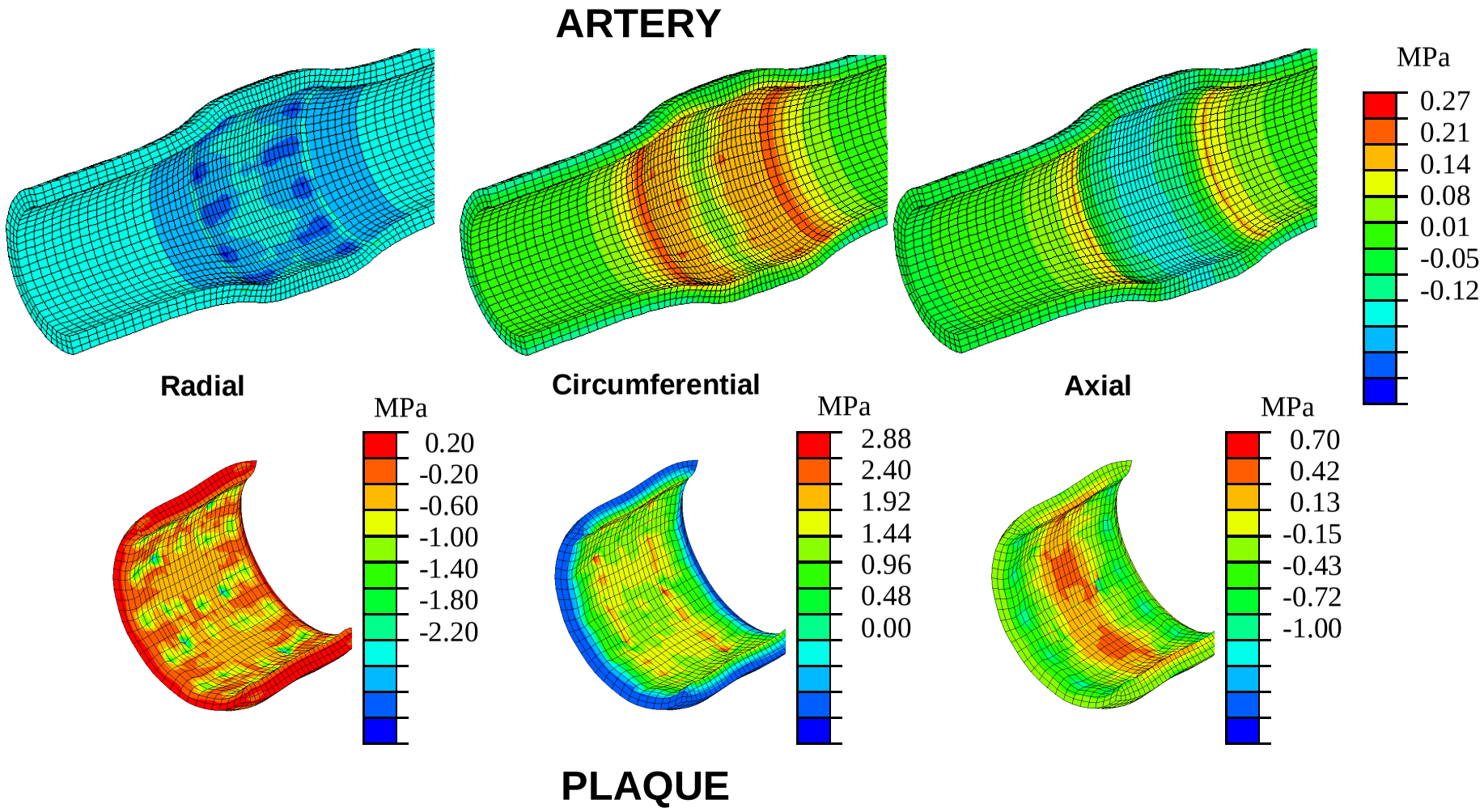
ARTERY
MPa
0.27
0.21
0.14
0.08
0.01
-0.05
-0.12
Radial
MPa
0.20
-0.20
-0.60
-1.00
-1.40
-1.80
-2.20
Circumferential
MPa
2.88
2.40
1.92
1.44
0.96
0.48
0.00
Axial
MPa
0.70
0.42
0.13
-0.15
-0.43
-0.72
-1.00
PLAQUE

Figure 4

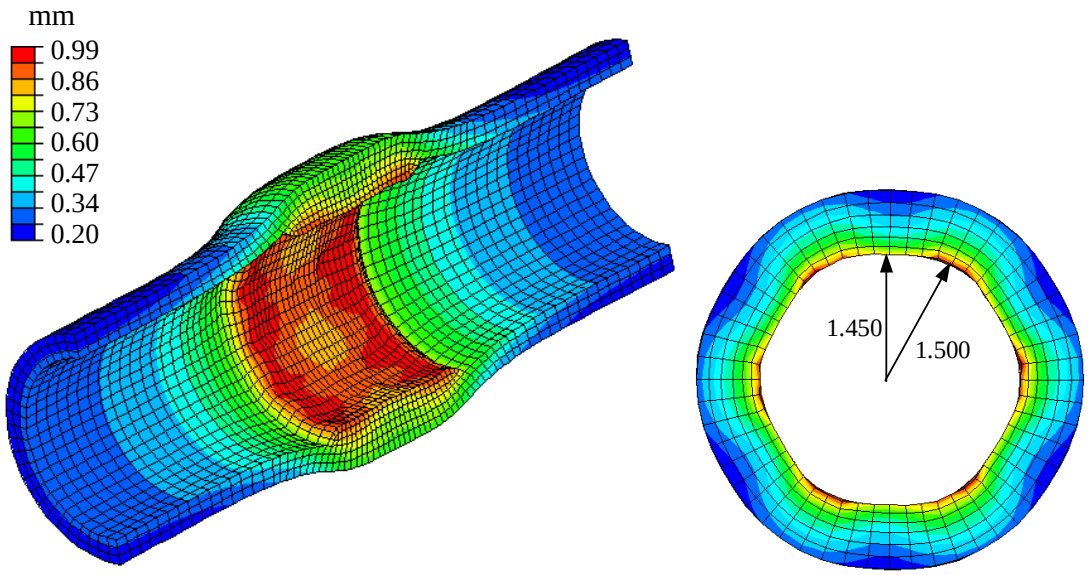


Figure 5

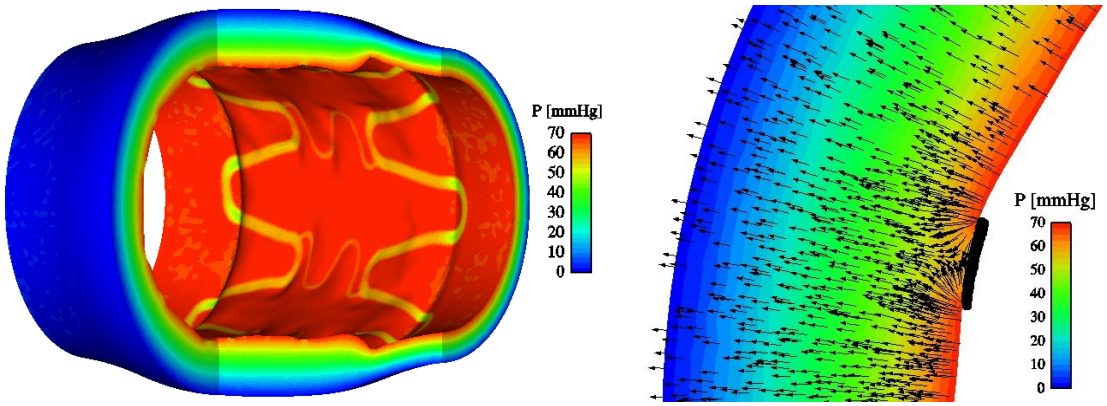


Figure 6

a)

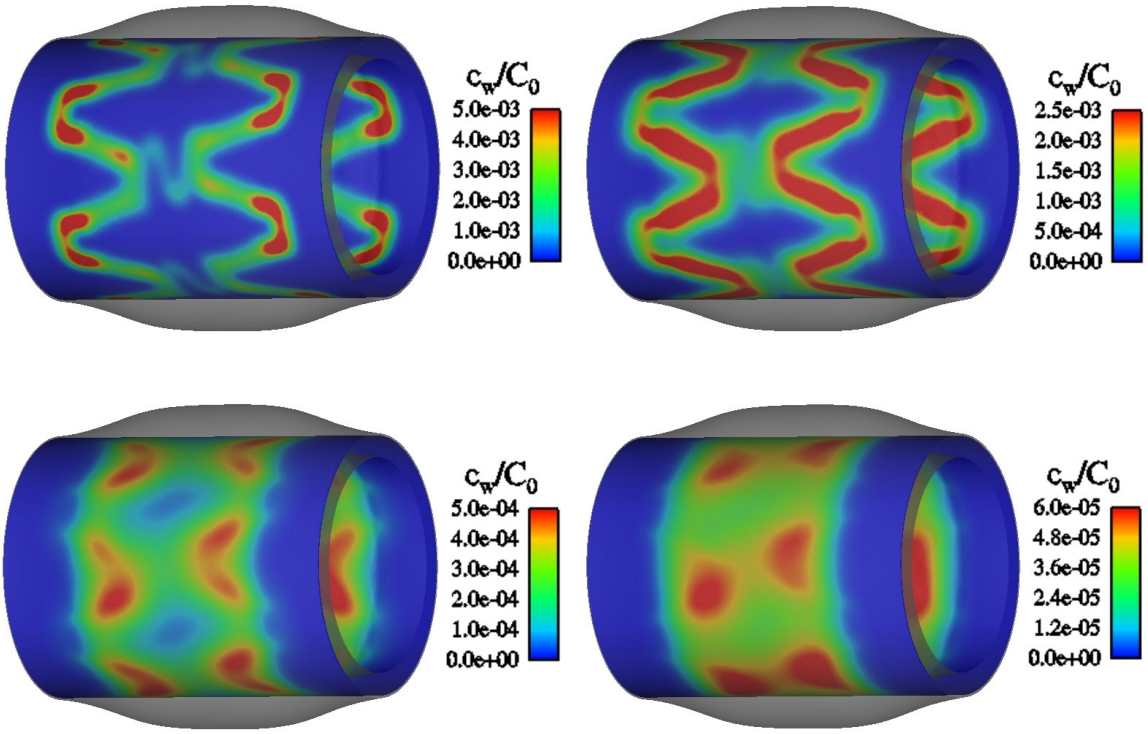
$c_w/C_0$
5.0e-03
4.0e-03
3.0e-03
2.0e-03
1.0e-03
0.0e+00
$c_w/C_0$
2.5e-03
2.0e-03
1.5e-03
1.0e-03
5.0e-04
0.0e+00
$c_w/C_0$
5.0e-04
4.0e-04
3.0e-04
2.0e-04
1.0e-04
0.0e+00
$c_w/C_0$
6.0e-05
4.8e-05
3.6e-05
2.4e-05
1.2e-05
0.0e+00

b)

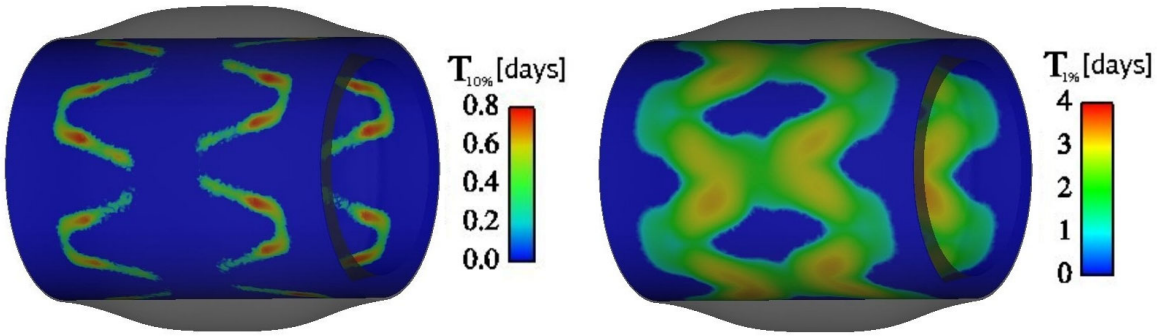
$T_{10\%}$[days]
0.8
0.6
0.4
0.2
0.0
$T_{1\%}$[days]
4
3
2
1
0

c)

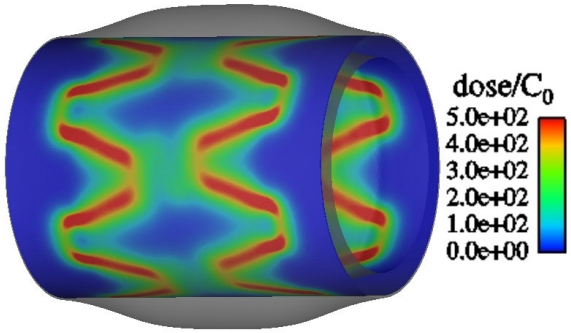
dose/$C_0$
5.0e+02
4.0e+02
3.0e+02
2.0e+02
1.0e+02
0.0e+00

Figure 7

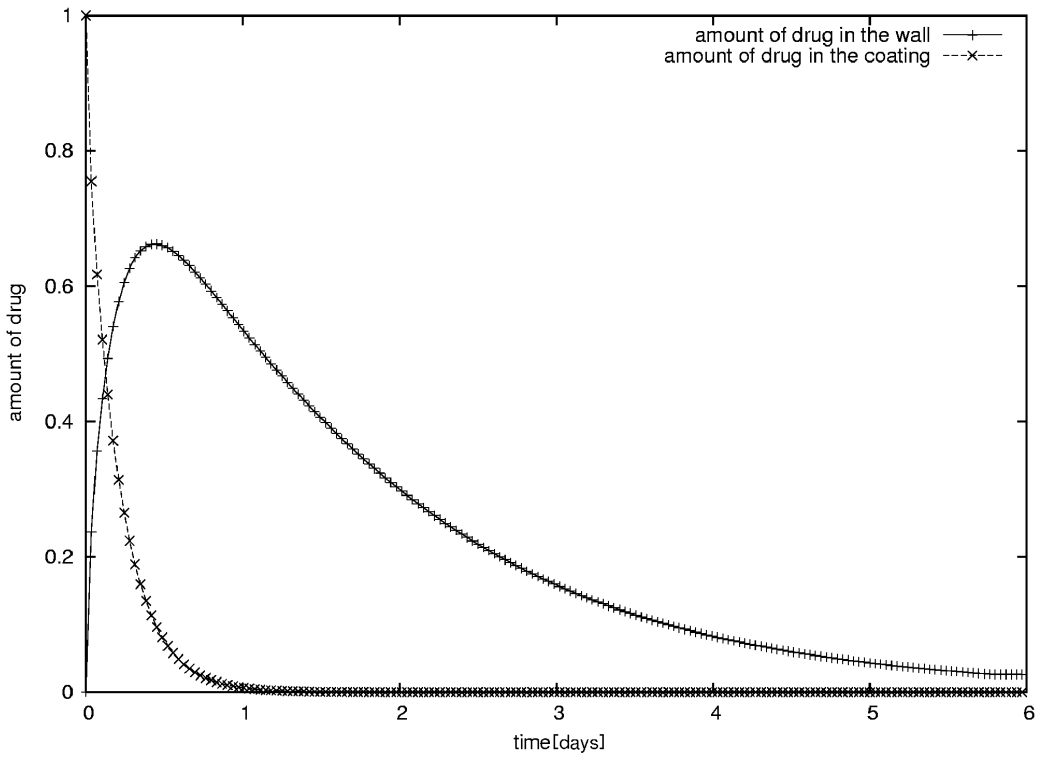
amount of drug in the wall
amount of drug in the coating
amount of drug
time[days]
0
0.2
0.4
0.6
0.8
1
0
1
2
3
4
5
6

Figure 8